



HHS Public Access

Author manuscript

Neuroscience. Author manuscript; available in PMC 2019 January 15.

Published in final edited form as:

Neuroscience. 2018 January 15; 369: 192–201. doi:10.1016/j.neuroscience.2017.11.017.

Neurotrophin and FGF signaling adapter proteins, FRS2 and FRS3, regulate dentate granule cell maturation and excitatory synaptogenesis

Sayan Nandi^{1,2}, Karina Alviña^{1,3,*}, Pablo J. Lituma^{1,*}, Pablo E. Castillo¹, and Jean M. Hébert^{1,2}

¹Department of Neuroscience, Albert Einstein College of Medicine, Bronx, NY, 10461, USA

²Department of Genetics, Albert Einstein College of Medicine, Bronx, NY, 10461, USA

³Department of Biological Sciences, Texas Tech University, Lubbock, TX, 79409, USA

Abstract

Dentate granule cells (DGCs) play important roles in cognitive processes. Knowledge about how growth factors such as FGFs and neurotrophins contribute to the maturation and synaptogenesis of DGCs is limited. Here, using brain-specific and germline mouse mutants we show that a module of neurotrophin and FGF signaling, the FGF Receptor Substrate (FRS) family of intracellular adapters, FRS2 and FRS3, are together required for postnatal brain development. In the hippocampus, FRS promotes dentate gyrus morphogenesis and DGC maturation during developmental neurogenesis, similar to previously published functions for both neurotrophins and FGFs. Consistent with a role in DGC maturation, two-photon imaging revealed that *Frs2,3*-double mutants have reduced numbers of dendritic branches and spines in DGCs. Functional analysis further showed that double mutant mice exhibit fewer excitatory synaptic inputs onto DGCs. These observations reveal roles for FRS adapters in DGC maturation and synaptogenesis and suggest that FRS proteins may act as an important node for FGF and neurotrophin signaling in postnatal hippocampal development.

Keywords

FRS; FGF; neurotrophin; hippocampus; neurogenesis; synaptogenesis

Corresponding authors: Jean M. Hébert, jean.hebert@einstein.yu.edu, Sayan Nandi, sayan.nandi@einstein.yu.edu, Departments of Neuroscience and Genetics, Albert Einstein College of Medicine, Bronx, NY.

*These authors contributed equally

Publisher's Disclaimer: This is a PDF file of an unedited manuscript that has been accepted for publication. As a service to our customers we are providing this early version of the manuscript. The manuscript will undergo copyediting, typesetting, and review of the resulting proof before it is published in its final citable form. Please note that during the production process errors may be discovered which could affect the content, and all legal disclaimers that apply to the journal pertain.

Conflict of Interest

Authors declare no conflict of interest.

Author Contributions

S.N., designed research, performed experiments, analyzed and interpreted data, and prepared manuscript; K.A., designed research, performed experiments, analyzed and interpreted data, and helped with manuscript preparation; P.J.L., designed research, performed experiments, analyzed and interpreted data, and helped with manuscript preparation; P.E.C., analyzed and interpreted data, and prepared manuscript; J.M.H., analyzed and interpreted data, and prepared manuscript.

Introduction

The hippocampal formation consists of complex arrays of neuronal circuits that act as a gateway of information acquisition and a center for information processing and storage (Andersen et al., 1971; Neves et al., 2008). The dentate gyrus (DG) is a unique hippocampal structure in that new neurons, dentate granule cells (DGCs), are generated and integrated into the circuitry throughout life, although at a much higher rate in the first two weeks after birth than later in adulthood (Anacker and Hen, 2017; Bischofberger, 2007; Deng et al., 2010; Gonçalves et al., 2016; Kemperman et al., 2015; Toni and Schinder, 2015). In contrast to hippocampal pyramidal neurons that are generated embryonically from the dorsomedial ventricular zone, DGCs are first generated in the dentate matrix during the first week of birth (Altman and Bayer, 1990; Super et al., 1998). The burst of DGC generation and concomitant cell death occur during the first two postnatal weeks, with the attainment of an overall functional maturity by the third week after birth, although some dendritic maturation and spine formation can continue beyond the first postnatal month (Gould et al., 1991; Gu et al., 2012; Laplagne et al., 2006; Liu et al., 1996; Lopez-Rojas and Kreutz, 2016; Mongiat et al., 2009; Zhao et al., 2006). DGC generation, maturation, and circuit integration have been implicated in cognitive functions involving pattern separation and completion, contextual and spatial memory, as well as neuropsychiatric disorders such as anxiety and depression (Nakashiba et al., 2012; Ryan et al., 2015; Sahay et al., 2007; Tonegawa et al., 2015; Weeden et al., 2015). Although the regulation of adult born DGC generation has received much attention, less is known about what regulates developmentally generated DGCs.

Growth factor signaling has been implicated in neurodevelopmental, neurodegenerative, and psychiatric disorders (Dode et al., 2003; Dubourg et al., 2016; Fu et al., 2016; Lu et al., 2013; Turner et al., 2012). Growth factors can play neurodevelopmental roles by altering the proliferative capacity and lineage potential of neural stem cells as well as by promoting neurogenesis, dendritogenesis, and neuronal migration (Doetsch et al., 2002; Licht et al., 2010; Pozas and Ibanez, 2005). In other cases, growth factor signals in the postnatal and adult brain regulate spinogenesis, synaptogenesis, synaptic strength, and activity-dependent synaptic plasticity (Kelleher et al., 2004; Patterson et al., 1996; Zhu et al., 2016). Lastly, certain factors such as neurotrophins and FGFs can play both neurogenic and synaptic roles (Dabrowski et al., 2015; Danzer et al., 2008; Li et al., 2008; Ohkubo et al., 2004).

Neurotrophins and FGFs promote postnatal dentate neurogenesis by signaling through their specific receptor subtypes, FGF Receptor 1 (FGFR1) and Neurotrophic Receptor Tyrosine Kinase 2 (NTRK2 or TRKB), respectively (Li et al., 2008; Ohkubo et al., 2004). Specific FGF receptor isoforms (FGFR1b and FGFR2b) were further involved in synaptogenesis in CA3 pyramidal neurons, while TRKB was implicated in DGC maturation (Dabrowski et al., 2015; Danzer et al., 2008). The mechanisms that mediate neurotrophin and FGF signals, however, remain unclear. The FRS proteins are one of the first-identified intracellular signaling adapters that transduce signals from both neurotrophin and FGF receptors (Dixon et al., 2006; Gotoh, 2008; Hadari et al., 2001; Meakin et al., 1999; Nandi et al., 2017). Although FRS was shown to be nonessential for TRKB-mediated, activity-dependent, long-

term plasticity in hippocampal CA1 (Minichiello et al., 2002), its roles in the context of hippocampal development, neuronal maturation, and synaptogenesis are unknown.

Using brain-specific and germline mutants, we show that FRS adapters are required for neural stem cell proliferation, DGC maturation, and DG morphogenesis during hippocampal development. Our results further suggest important roles for FRS in excitatory synaptogenesis in developmentally-generated DGCs.

Experimental procedures

Mice

The experiments described in this study were approved by the IACUC of the Albert Einstein College of Medicine. *hGFAP-Cre* (Zhuo et al., 2001), *Frs2^{fl}* (Lin et al., 2007) and *Frs3^{-/-}* (Nandi et al., 2017) mice were maintained and genotyped as previously described.

Histology and immunohistochemistry (IHC)

P7 brains were fixed with 4% paraformaldehyde (PFA) in PBS (overnight, 4°C), followed by paraffin-embedding. Five µm thick sections were stained with hematoxylin and eosin (H&E), or were immunostained with Ki67 antibodies. For all other IHC experiments, P7 brains were incubated with 4% PFA in PBS (6 h, 4°C) and in 10% (4 hours) and 20% (overnight) sucrose in PBS (4°C), and embedded in O.C.T. Fourteen µm thick cryosections were then immunostained. IHC sections were either mounted with Prolong-diamond antifade-mounting media with DAPI (Invitrogen) (frozen sections) or counterstained with hematoxylin (paraffin sections) and imaged using a Zeiss fluorescent microscope with Axiovision software. Total hippocampal, CA neuronal and DGC field areas were calculated after importing 5× and 40× H&E images taken from equivalent sagittal planes from serially cut sections, followed by contouring and analyzing absolute areas using Image J software. Antibody dilutions (IHC): Ki67, rabbit monoclonal, 1:400 (Cell Signaling); active caspase-3, rabbit polyclonal, 1:200 (Cell Signaling); GFAP, rabbit polyclonal, 1:500 (Dako) or mouse monoclonal, 1:400 (SIGMA); DCX, guinea pig polyclonal, 1:500 (Millipore); TBR2, rabbit polyclonal, 1:500, (Abcam); NeuN, mouse monoclonal Alexafluor-488, 1:100 (Millipore); Cre, rabbit polyclonal, 1:1000 (abcam).

Hippocampal slice preparation

Acute hippocampal slices (300 µm thick) from P21–P25 control and mutant mice were prepared without differentiation of sex. Runts (see below) were excluded from electrophysiology and imaging experiments. Hippocampi were dissected and sectioned using a VT1200s vibratome (Leica Microsystems Co.) or a DTK-2000 microslicer (Dosaka EM) in a chilled solution (cutting solution) containing 215 mM sucrose, 2.5 mM KCl, 26 mM NaHCO₃, 1.6 mM NaH₂PO₄, 1 mM CaCl₂, 4 mM MgCl₂, 4 mM MgSO₄ and 20 mM glucose. Slices were collected and placed in a chamber with 1:1 cutting solution and artificial cerebrospinal fluid (ACSF) or recording solution containing 124 mM NaCl, 2.5 mM KCl, 26 mM NaHCO₃, 1 mM NaH₂PO₄, 2.5 mM CaCl₂, 1.3 mM MgSO₄ and 10 mM glucose at room temperature. After 10 minutes, the cutting/recording solution mixture was gradually replaced with 100% recording solution. All solutions were equilibrated with 95%

O₂ and 5% CO₂ (pH 7.4). Slices were incubated for a recovery time of at least 30 minutes before recording and imaging.

Electrophysiology

Miniature excitatory postsynaptic currents (mEPSCs) were recorded at $32^{\circ} \pm 1^{\circ}\text{C}$ in a submersion-type recording chamber perfused at ~ 2 ml/min with ACSF supplemented with the voltage-gated Na⁺ channel blocker TTX (0.5 μM) to block action potentials, and the GABA_A receptor antagonist picrotoxin (100 μM) to block fast inhibitory transmission. Whole-cell patch-clamp recordings were done using a Multiclamp 700B amplifier (Molecular Devices) from DGCs voltage clamped at -65 mV using patch-type pipette electrodes (3–4 M Ω) containing: 131 mM cesium gluconate, 8 mM NaCl, 1 mM CaCl₂, 10 mM EGTA, 10 mM glucose, 10 mM HEPES and 0.03 mM Alexa Fluor-594 (pH 7.2, 285–290 mOsm) unless specified otherwise. Series resistance (20–30 M Ω) was monitored throughout all experiments using a -5 mV, 50 ms voltage step, cells that exhibited a $>20\%$ series resistance change were excluded from analysis. Immature DGCs were avoided by visually selecting and patching cells at least 30 μm above the hilar border and excluding cells with an input resistance >1 G Ω . Mini-Analysis software (Synaptosoft) was used to determine amplitude and frequency of mEPSCs with a threshold set to 5 pA. For extracellular field recordings, a stimulating patch-type pipette filled with ACSF was placed in the middle third of the dentate gyrus molecular layer in order to activate the medial perforant path. A recording patch-type pipette containing 1 M NaCl or ACSF was placed ~ 200 μm away in the medial molecular layer at similar slice depth (~ 200 μm). To elicit synaptic responses paired, monopolar, square-wave current pulses (100 μs pulse width) were delivered through a stimulus isolator (Isoflex, AMPI). Extracellular field recordings were performed at 26° 1°C in the absence of any drug. Paired-pulse ratio (PPR) was calculated by dividing the amplitude of the second pulse by the first pulse (P_2/P_1) at a 100-ms inter-stimulus interval.

Two-photon imaging and analyses of dendrites and spines

After 20 minutes of recording synaptic events, DGCs patch-loaded with Alexa Fluor-594 (30 μM) were imaged using an Ultima In Vitro two-photon laser scanning fluorescence microscope (Bruker Corporation) with a 60 \times fluor objective (NA = 1.00, Nikon) and an Insight Deep See Laser (Spectra Physics) tuned to 830 nm. Z-stack images of the dendritic tree of DGCs were collected at a 512×512 pixel resolution at a 1.0 \times magnification. Higher magnification (4.0 \times and 8.0 \times) and higher resolution (1280×1280 pixel) images were acquired 50 μm from soma to quantify changes in dendritic spine density. Three-dimensional reconstructions of DGC dendritic trees were analyzed using NeuroLucida neuron tracing software (11.07 64-bit) (MBF bioscience, Williston, USA). Sholl analyses were carried out using 40 μm concentric circular bins from soma while dendritic spine density was assessed by the Image J software (Bicanic et al., 2017; Sholl, 1953; Smith et al., 2009).

Chemicals & Drugs

All chemicals used for ACSF and intracellular solutions were acquired from Sigma-Aldrich (St. Louis, MO). For mEPSC recordings, TTX was purchased from Cayman Chemical Co. (Ann Arbor, MI) and picrotoxin from Sigma-Aldrich (St. Louis, MO). Alexa Fluor-594 was

ordered from ThermoFisher Sci. (Waltham, MA) and added to intracellular solution to a final concentration of 30 μ M prior to patch-clamp recordings and imaging.

Statistical analyses

Unpaired t-test was performed on experiments that determined changes in morphogenesis, maturation, dendritic length and spine density. For dendritic arborization, two-way ANOVA (significance set to $p = 0.05$) and for electrophysiological experiments (mEPSCs and PPR measurements), one-way ANOVA (significance set to $p = 0.05$) was performed. Experimenters were blind to control and mutant genotypes during patch-loading and electrophysiological recordings.

Results

FRS adapters are required for the maintenance of body weight and survival in one-third of mutant mice

To address the roles for FRS proteins in dorsal forebrain development, we simultaneously ablated FRS2 and FRS3 by combining a conditional knockout of a floxed *Frs2* allele (*hGFAP-Cre* driven) and a germ-line deletion *Frs3* mutant (Fig. 1A; Lin et al., 2007; Nandi et al., 2017; Zhuo et al., 2001). *hGFAP-Cre* is active within multipotent neural stem cells at E13.5 and largely restricted to the dorsal telencephalon, resulting in efficient targeting of postnatal and adult cortical neurons and astrocytes, including hippocampal CA and DG fields, but excluding interneurons and astrocytes located specifically in the hilar and CA1 regions (Ohkubo et al., 2004; Zhuo et al., 2001). Consistent with these previous reports, early postnatal *hGFAP*-driven Cre expression was observed in neural stem cells, which leads to inheritance of recombined alleles in all their neuronal and glial progeny, and astrocytes (Fig. 2). Importantly, the pattern of expression is not affected by loss of FRS3 since no detectable difference is observed between *Frs3*^{+/-} controls and *Frs3*^{-/-} mutants (Fig. 2).

Although two thirds of *hGFAP-Cre;Frs2*^{fl/fl};*Frs3*^{-/-} (double mutant) mice exhibited normal body weights compared with control mice at postnatal day 20 (P20), the remaining third were runts (Fig. 1B), resulting in an overall slightly smaller body weight for mutants (control: 14.6 ± 0.5 g, vs. mutant: 12.3 ± 1.0 g, average \pm SEM; $n=9$; $p=0.05$). The average differences in body weight between control and mutant groups disappeared by P30 (control: 22.2 ± 1.4 g, vs. mutant: 20.2 ± 2.9 g, average \pm SEM; $n=5$; $p=0.6$) due to death of 13.3% of the runts between P20 and P30 (Fig. 1B). The other 20% of runts survived until P60–P75. The cause for the lack of weight gain and death remains undetermined. Mutant mice with normal body weights appeared healthy and survived into adulthood.

FRS adapters are together required for early postnatal brain development

The generation of developmentally-generated DGCs primarily begins after birth and peaks at P14, after which neurogenesis greatly declines to the lower levels observed for adult-born DGCs (Altman and Bayer, 1990; Super et al., 1998; Anacker and Hen, 2017; Bischofberger, 2007; Deng et al., 2010; Gonçaves et al., 2016; Kemperman et al., 2015; Toni and Schinder, 2015). Therefore, we chose to examine the midpoint of developmental DGC neurogenesis at P7. Examination of the brains of both single and double mutants and control littermates at

this age revealed that double mutant mice had a shorter cortical length along the A/P axis (~25% reduction compared with control or *Frs2* single mutants) (Fig. 3) and *Frs3* single mutants had ~8% reduction in cortical length (Fig. 3). Both *Frs3* single mutants and double mutants showed cerebellar foliation deficits at P7 (Fig. 3C). These results suggest that FRS2 and FRS3 can to some extent compensate for each other during postnatal brain development, similar to our earlier observations in embryonic telencephalon development (Nandi et al., 2017).

Double mutants also displayed a disproportionately smaller hippocampus, despite overall normal hippocampal patterning and largely normal neocortical thickness (Fig. 3A,B and 4A,B). Specifically, DG morphology was abnormal with a 45% reduction in the DGC cell body layer thickness in mutants ($p=0.02$) (Fig. 4E,F), recapitulating *Fgfr1* and *TirkB* single mutant phenotypes, further suggesting a specific role for FRS in the DG (Li et al., 2008; Ohkubo et al., 2004). The CA1 pyramidal cell layer thickness was largely unaffected in mutants ($p=0.61$) (Fig. 4C,D). The DG morphogenesis deficits were absent in either *Frs2*, or *Frs3* single mutants (Fig. 3B). These observations suggest that FRS2 and FRS3 together transmit some FGF and/or neurotrophin signaling during dorsal forebrain development with a critical role in the formation of the hippocampal DG.

FRS adapters regulate developmental hippocampal neurogenesis

To assess whether FRS proteins play a role in DG neurogenesis, we performed immunostaining in P7 control and double mutant brain sections using markers for proliferation (Ki67), cell death (active caspase-3), neural stem cells (GFAP), immature neurons (TBR2, DCX) and mature neurons (NeuN). Mutants exhibited a reduction in cellular proliferation, evidenced by fewer Ki67+ cells ($p=0.04$), without affecting cellular survival ($p=0.85$) in the DG (Fig. 5A–B, F–G), which was very low, consistent with previous reports (e.g. Favaro et al., 2009). Furthermore, the number of neural stem cells was reduced ($p=0.03$) in mutant mice (Fig. 5C,H), although the number of immature neurons was not significantly reduced ($p=0.56$) in mutant mice (Fig. 5D,I). The distribution of immature neurons in the DG was abnormal in mutant mice suggesting that loss of FRS resulted in an altered maturation of DGCs (Fig. 5D,I). Consistent with altered maturation, the number of mature DGCs was significantly reduced ($p=0.002$) in mutant mice (Fig. 5E,J).

FRS adapters promote DGC maturation

To further investigate the role of FRS in DGC maturation, we performed Sholl analyses of dendrites by analyzing two-photon images of dye-filled DGCs in acute hippocampal slices at P21–P25. Double mutant mice which had lower body weights at P20 were excluded from analysis. Consistent with a role in maturation, DGCs in mutant mice displayed a modest but significant decrease in the complexity of their dendritic trees ($p=0.04$), suggesting DGC maturational deficits in mutant mice (Fig. 6A,B). The total length of the dendrites was also reduced ($p=0.02$) in mutant mice (Fig. 6C), further suggesting a role for FRS in DGC dendritogenesis. Together these observations suggest that FRS promotes neural stem cell proliferation, as well as DGC maturation in the postnatal DG.

FRS adapters are required for excitatory DGC synaptogenesis

To investigate whether FRS plays a role in synaptogenesis, we assessed dendritic spine density and excitatory transmission in mature DGCs in P21–P25 control and mutant mice. Mutant DGCs exhibited a strong reduction ($p=0.0009$) in dendritic spine density, quantified from two-photon imaging of patched DGCs loaded with Alexa Fluor-594 (Fig. 7A). To test whether these deficits in DGC dendritic spines could affect synaptogenesis in mutants, we compared spontaneous excitatory transmission in control and mutant mice. Consistent with a reduction in DGC dendritic spine density, whole-cell voltage-clamp recordings showed that the frequency ($p=0.009$) but not amplitude ($p=0.15$) of mEPSCs was reduced in mutant DGCs (Fig. 7B,C). Extracellular field recordings of stimulated medial perforant path synapses onto DGCs further revealed that loss of FRS did not affect presynaptic release probability as measured by paired-pulse ratio (PPR control: 0.9 ± 0.07 ; PPR mutant: 1.0 ± 0.06 ; average \pm SEM; $p=0.29$; at least five slices from three mice per genotype), suggesting that decreased neurotransmitter release was unlikely to play a role in the reduction of mEPSC frequency in mutant mice. Together these observations suggest that FRS plays a role in the development of functional synapses in DGCs.

Discussion

Here we demonstrate important roles for a family of adapters, the FRS proteins, which are dedicated to neurotrophin and FGF signaling, in developmental neurogenesis in the hippocampus, as well as in dendritogenesis in developmentally-generated DGCs (Fig. 3–6). These adapters were also required to promote DGC dendritic spinogenesis and excitatory synaptogenesis involving DGCs (Fig. 7). While alterations in neurogenesis are linked to mental illnesses such as anxiety and depression (David et al., 2009; Hill et al., 2015; Li et al., 2008), alterations in spinogenesis are implicated in neurodevelopmental and psychiatric illnesses including autism-spectrum disorders, schizophrenia, and frontotemporal dementia (Chen et al., 2012; Sweet et al., 2009; Wang et al., 2011). In our study, we could not rule out the possibility of astrocyte-mediated effects for these adapters in the regulation of synaptogenesis since astrocytes are also targeted by *hGFAP-Cre* and express *Fgfr* genes (Kang et al., 2014; Sultan et al., 2015; Zhuo et al., 2001). In addition, enhanced pruning could potentially also explain a reduced spine density in *Frs* mutants. Whether FRS indeed plays a direct role in synaptic physiology remains to be determined. Whether loss of FRS can contribute to neuropathological conditions also remains an open question.

Relevant to the direct roles of FRS in DGC synaptogenesis, we observed a reduction in mEPSC frequency (~58%), which can be explained by a reduction (~47%) in postsynaptic (DGC) spine density in mutant mice (Fig. 7). Although a deficit in presynaptic function could potentially contribute to a reduction in mEPSC frequency, the lack of change in paired-pulse ratio in mutant mice makes this possibility highly unlikely. Consistent with this observation, *Frs2* and *Frs3* expression is significantly stronger in postsynaptic DGCs compared with presynaptic inputs from the entorhinal cortex in the adult brain (Allen Brain Atlas).

Although the double *Frs* mutants described in this study could be used to examine changes in activity-dependent, long-term plasticity, given the developmental synaptic deficits that

were characterized, interpreting whether effects on plasticity were directly due to an involvement of FRS in plasticity or indirectly involved due to the developmental defects would not be distinguishable. Although FRS was previously shown to be dispensable in TRKB-mediated long-term potentiation in CA1, it was required for TRKB-mediated, activity-dependent, long-term changes in amygdala (Minichiello et al., 2002; Musumeci et al., 2009). In addition, recent studies have implicated FGF signaling in long-term plasticity in the DG as well as in CA1 (Dallerac et al., 2011; Knafo et al., 2012; Uchida et al., 2017). In these studies, however, the possibility of astrocyte-mediated, FGF/FRS-dependent long-term changes was not ruled out. Future work will address specifically for neurons the direct roles for FRS and/or other adapters in FGF-dependent, activity-dependent, long-term plasticity.

While roles for neurotrophin and FGF signaling in neurogenesis are in line with traditional functions for these pathways, we observed somewhat unexpected and underexplored roles for FRS-mediated signaling pathways in dendritogenesis and spinogenesis. While it is possible that a deficit in the maturation of DGCs might have in part contributed to the reduced synaptogenesis in mutant mice (Andreae et al., 2012; Hsia et al., 1998), our results raise the possibility that FRS, independent of its roles in neurogenesis and DGC maturation, could play direct roles in spine formation and/or stabilization in mature DGCs. For example, neurotrophin signaling via MAPK/PI3K could enhance dendritic complexity and spine density in mature neurons (Kumar et al., 2005; McAllister et al., 1995).

Triple mutants in which *Fgfr1*, *Fgfr2*, and *Fgfr3* were deleted from neural stem cells using the same *hGFAP-Cre* driver as in this study displayed a dramatic reduction in cortical thickness due to premature neural stem cell differentiation (Kang et al., 2009). In contrast, *Frs* mutant mice described here had largely normal cortical thickness, suggesting that other adapters are responsible for FGFR-dependent regulation of cortical stem cells (Fig. 3A, 4A). On the other hand, *Fgfr1* or *TrkB* are independently required for the maintenance of hippocampal size and neural stem cell proliferation in the DG (Li et al., 2008; Ohkubo et al., 2004), suggesting that both are independently required to sufficiently activate signal transduction through FRS in DG stem cells. Interestingly, both *Fgfr1* and *TrkB* (but not the other FGF and neurotrophin receptors) are strongly expressed in the dentate SGZ harboring neural stem cells, with a dramatically reduced expression of *Fgfr1* (but not *TrkB*) in granule cell layers of the adult hippocampus (Bansal et al., 2003; Allen Brain Atlas). In contrast, *Frs2* and *Frs3* are uniformly expressed throughout the SGZ and granule cell layers (Allen Brain Atlas). The differential expression pattern between *Fgfr1* and *Frs2/Frs3* suggests FGF-dependent as well as FGF-independent roles for FRS in the DG.

Finally, although the *Frs2/Frs3* phenotypes described here suggest a role for FRS adapter proteins in mediating FGF and neurotrophin signaling in the developing hippocampus, we can not at this time exclude the possibility that FRS mediates additional or alternative signals. FRS has been shown to bind other tyrosine kinase receptors including RET, ALK, and EGF receptors (Degoutin et al., 2007; Huang et al., 2006; Kurokawa et al., 2001), albeit *in vivo* evidence for such interactions have not been shown. Although these receptors have not been implicated in the hippocampal processes described here, they have been implicated in other CNS processes, including development, plasticity, behavior, neuroprotection, and

tumorigenesis (Araujo et al., 1997; Bilsland et al., 2008; Guo et al., 2017). Therefore, additional roles for FRS are anticipated, including potentially in the developing hippocampus.

Acknowledgments

This work has been supported by NIH grants MH070596 and NS088943 to J.M.H., MH081935 and DA017392 to P.E.C., and F31 MH109267 to P.J.L. We thank Marta Gronska for critically reading and editing the manuscript.

References

- Altman J, Bayer SA. Migration and distribution of two populations of hippocampal granule cell precursors during the perinatal and postnatal periods. *J Comp Neurol.* 1990; 301:365–381. [PubMed: 2262596]
- Anacker C, Hen R. Adult hippocampal neurogenesis and cognitive flexibility - linking memory and mood. *Nat Rev Neurosci.* 2017; 18:335–346. [PubMed: 28469276]
- Andersen P, Bliss TV, Skrede KK. Lamellar organization of hippocampal pathways. *Exp Brain Res.* 1971; 13:222–238. [PubMed: 5570425]
- Andreae LC, Fredj NB, Burrone J. Independent vesicle pools underlie different modes of release during neuronal development. *J Neurosci.* 2012; 32:1867–1874. [PubMed: 22302825]
- Araujo DM, Hilt DC, Miller PJ, Wen D, Jiao S, Lapchak PA. ret receptor tyrosine kinase immunoreactivity is altered in glial cell line-derived neurotrophic factor-responsive neurons following lesions of the nigrostriatal and septohippocampal pathways. *Neuroscience.* 1997; 80:9–16. [PubMed: 9252216]
- Bansal R, Lakhina V, Remedios R, Tole S. Expression of FGF receptors 1, 2, 3 in the embryonic and postnatal mouse brain compared with *Pdgfra*, *Olig2* and *Plp/dm20*: implications for oligodendrocyte development. *Dev Neurosci.* 2003; 25:83–95. [PubMed: 12966207]
- Bicanic I, Hladnik A, Petanjek Z. A Quantitative Golgi Study of Dendritic Morphology in the Mice Striatal Medium Spiny Neurons. *Front Neuroanat.* 2017; 11:37. [PubMed: 28503136]
- Bilsland JG, Wheeldon A, Mead A, Znamenskiy P, Almond S, Waters KA, Thakur M, Beaumont V, Bonnert TP, Heavens R, Whiting P, McAllister G, Munoz-Sanjuan I. Behavioral and neurochemical alterations in mice deficient in anaplastic lymphoma kinase suggest therapeutic potential for psychiatric indications. *Neuropsychopharmacology.* 2008; 33:685–700. [PubMed: 17487225]
- Bischofberger J. Young and excitable: new neurons in memory networks. *Nat Neurosci.* 2007; 10:273–275. [PubMed: 17318218]
- Chen YK, Chen CY, Hu HT, Hsueh YP. CTTNBP2, but not CTTNBP2NL, regulates dendritic spinogenesis and synaptic distribution of the striatin-PP2A complex. *Mol Biol Cell.* 2012; 23:4383–4392. [PubMed: 23015759]
- Dabrowski A, Terauchi A, Strong C, Umemori H. Distinct sets of FGF receptors sculpt excitatory and inhibitory synaptogenesis. *Development.* 2015; 142:1818–1830. [PubMed: 25926357]
- Dallerac G, Zerwas M, Novikova T, Callu D, Leblanc-Veyrac P, Bock E, Berezin V, Rampon C, Doyere V. The neural cell adhesion molecule-derived peptide FGL facilitates long-term plasticity in the dentate gyrus in vivo. *Learn Mem.* 2011; 18:306–313. [PubMed: 21508096]
- Danzer SC, Kotloski RJ, Walter C, Hughes M, McNamara JO. Altered morphology of hippocampal dentate granule cell presynaptic and postsynaptic terminals following conditional deletion of *TrkB*. *Hippocampus.* 2008; 18:668–678. [PubMed: 18398849]
- David DJ, Samuels BA, Rainer Q, Wang JW, Marsteller D, Mendez I, Drew M, Craig DA, Guiard BP, Guilloux JP, Artymyshyn RP, Gardier AM, Gerald C, Antonijevic IA, Leonardo ED, Hen R. Neurogenesis-dependent and -independent effects of fluoxetine in an animal model of anxiety/depression. *Neuron.* 2009; 62:479–493. [PubMed: 19477151]
- Degoutin J, Vigny M, Gouzi JY. ALK activation induces Shc and FRS2 recruitment: Signaling and phenotypic outcomes in PC12 cells differentiation. *FEBS Lett.* 2007; 581:727–734. [PubMed: 17274988]

- Deng W, Aimone JB, Gage FH. New neurons and new memories: how does adult hippocampal neurogenesis affect learning and memory? *Nat Rev Neurosci.* 2010; 11:339–350. [PubMed: 20354534]
- Dixon SJ, MacDonald JI, Robinson KN, Kubu CJ, Meakin SO. Trk receptor binding and neurotrophin/fibroblast growth factor (FGF)-dependent activation of the FGF receptor substrate (FRS)-3. *Biochim Biophys Acta.* 2006; 1763:366–380. [PubMed: 16697063]
- Dode C, Levilliers J, Dupont JM, De Paepe A, Le Du N, Soussi-Yanicostas N, Coimbra RS, Delmaghani S, Compain-Nouaille S, Baverel F, Pecheux C, Le Tessier D, Cruaud C, Delpech M, Speleman F, Vermeulen S, Amalfitano A, Bachelot Y, Bouchard P, Cabrol S, Carel JC, Delemarrevan de Waal H, Goulet-Salmon B, Kottler ML, Richard O, Sanchez-Franco F, Saura R, Young J, Petit C, Hardelin JP. Loss-of-function mutations in FGFR1 cause autosomal dominant Kallmann syndrome. *Nat Genet.* 2003; 33:463–465. [PubMed: 12627230]
- Doetsch F, Petreanu L, Caille I, Garcia-Verdugo JM, Alvarez-Buylla A. EGF converts transit-amplifying neurogenic precursors in the adult brain into multipotent stem cells. *Neuron.* 2002; 36:1021–1034. [PubMed: 12495619]
- Dubourg C, Carre W, Hamdi-Roze H, Mouden C, Roume J, Abdelmajid B, Amram D, Baumann C, Chassaing N, Coubes C, Faivre-Olivier L, Ginglinger E, Gonzales M, Levy-Mozziconacci A, Lynch SA, Naudion S, Pasquier L, Poidvin A, Prieur F, Sarda P, Toutain A, Dupe V, Akloul L, Odent S, de Tairac M, David V. Mutational Spectrum in Holoprosencephaly Shows That FGF is a New Major Signaling Pathway. *Hum Mutat.* 2016; 37:1329–1339. [PubMed: 27363716]
- Favaro R, Valotta M, Ferri AL, Latorre E, Mariani J, Giachino C, Lancini C, Tosetti V, Ottolenghi S, Taylor V, Nicolis SK. Hippocampal development and neural stem cell maintenance require Sox2-dependent regulation of Shh. *Nat Neurosci.* 2009; 12:1248–1256. [PubMed: 19734891]
- Fu AK, Hung KW, Yuen MY, Zhou X, Mak DS, Chan IC, Cheung TH, Zhang B, Fu WY, Liew FY, Ip NY. IL-33 ameliorates Alzheimer's disease-like pathology and cognitive decline. *Proc Natl Acad Sci U S A.* 2016; 113:E2705–2713. [PubMed: 27091974]
- Gonçalves JT, Schafer ST, Gage FH. Adult neurogenesis in the hippocampus: From stem cells to behavior. *Cell.* 2016; 167:897–914. [PubMed: 27814520]
- Gotoh N. Regulation of growth factor signaling by FRS2 family docking/scaffold adaptor proteins. *Cancer Sci.* 2008; 99:1319–1325. [PubMed: 18452557]
- Gould E, Woolley CS, McEwen BS. Naturally occurring cell death in the developing dentate gyrus of the rat. *J Comp Neurol.* 1991; 304:408–418. [PubMed: 2022756]
- Gu Y, Arruda-Carvalho M, Wang J, Janoschka SR, Josselyn SA, Frankland PW, Ge S. Optical controlling reveals time-dependent roles for adult-born dentate granule cells. *Nat Neurosci.* 2012; 15:1700–1706. [PubMed: 23143513]
- Guo G, Gong K, Ali S, Ali N, Shallwani S, Hatanpaa KJ, Pan E, Mickey B, Burma S, Wang DH, Kesari S, Sarkaria JN, Zhao D, Habib AA. A TNF-JNK-Axl-ERK signaling axis mediates primary resistance to EGFR inhibition in glioblastoma. *Nat Neurosci.* 2017; 20:1074–1084. [PubMed: 28604685]
- Hadari YR, Gotoh N, Kouhara H, Lax I, Schlessinger J. Critical role for the docking-protein FRS2 alpha in FGF receptor-mediated signal transduction pathways. *Proc Natl Acad Sci U S A.* 2001; 98:8578–8583. [PubMed: 11447289]
- Hill AS, Sahay A, Hen R. Increasing Adult Hippocampal Neurogenesis is Sufficient to Reduce Anxiety and Depression-Like Behaviors. *Neuropsychopharmacology.* 2015; 40:2368–2378. [PubMed: 25833129]
- Hsia AY, Malenka RC, Nicoll RA. Development of excitatory circuitry in the hippocampus. *J Neurophysiol.* 1998; 79:2013–2024. [PubMed: 9535965]
- Huang L, Watanabe M, Chikamori M, Kido Y, Yamamoto T, Shibuya M, Gotoh N, Tsuchida N. Unique role of SNT-2/FRS2beta/FRS3 docking/adaptor protein for negative regulation in EGF receptor tyrosine kinase signaling pathways. *Oncogene.* 2006; 25:6457–6466. [PubMed: 16702953]
- Hunt DL, Puente N, Grandes P, Castillo PE. Bidirectional NMDA receptor plasticity controls CA3 output and heterosynaptic metaplasticity. *Nat Neurosci.* 2013; 16:1049–1059. [PubMed: 23852115]

- Kang W, Wong LC, Shi SH, Hébert JM. The transition from radial glial to intermediate progenitor cell is inhibited by FGF signaling during corticogenesis. *J Neurosci*. 2009; 29:14571–14580. [PubMed: 19923290]
- Kang W, Balordi F, Su N, Chen L, Fishell G, Hébert JM. Astrocyte activation is suppressed in both normal and injured brain by FGF signaling. *Proc Natl Acad Sci U S A*. 2014; 111:E2987–2995. [PubMed: 25002516]
- Kelleher RJ 3rd, Govindarajan A, Jung HY, Kang H, Tonegawa S. Translational control by MAPK signaling in long-term synaptic plasticity and memory. *Cell*. 2004; 116:467–479. [PubMed: 15016380]
- Kempermann G, Song H, Gage FH. Neurogenesis in the adult hippocampus. *Cold Spring Harb Perspect Biol*. 2015; 7:a018812. [PubMed: 26330519]
- Knafo S, Venero C, Sanchez-Puelles C, Pereda-Perez I, Franco A, Sandi C, Suarez LM, Solis JM, Alonso-Nanclares L, Martin ED, Merino-Serrais P, Borcel E, Li S, Chen Y, Gonzalez-Soriano J, Berezin V, Bock E, Defelipe J, Esteban JA. Facilitation of AMPA receptor synaptic delivery as a molecular mechanism for cognitive enhancement. *PLoS Biol*. 2012; 10:e1001262. [PubMed: 22363206]
- Kumar V, Zhang MX, Swank MW, Kunz J, Wu GY. Regulation of dendritic morphogenesis by Ras-PI3K-Akt-mTOR and Ras-MAPK signaling pathways. *J Neurosci*. 2005; 25:11288–11299. [PubMed: 16339024]
- Kurokawa K, Iwashita T, Murakami H, Hayashi H, Kawai K, Takahashi M. Identification of SNT/FRS2 docking site on RET receptor tyrosine kinase and its role for signal transduction. *Oncogene*. 2001; 20:1929–1938. [PubMed: 11360177]
- Laplagne DA, Esposito MS, Piatti VC, Morgenstern NA, Zhao C, van Praag H, Gage FH, Schinder AF. Functional convergence of neurons generated in the developing and adult hippocampus. *PLoS Biol*. 2006; 4:e409. [PubMed: 17121455]
- Li Y, Luikart BW, Birnbaum S, Chen J, Kwon CH, Kernie SG, Bassel-Duby R, Parada LF. TrkB regulates hippocampal neurogenesis and governs sensitivity to antidepressive treatment. *Neuron*. 2008; 59:399–412. [PubMed: 18701066]
- Licht T, Eavri R, Goshen I, Shlomai Y, Mizrahi A, Keshet E. VEGF is required for dendritogenesis of newly born olfactory bulb interneurons. *Development*. 2010; 137:261–271. [PubMed: 20040492]
- Lin Y, Zhang J, Zhang Y, Wang F. Generation of an Frs2alpha conditional null allele. *Genesis*. 2007; 45:554–559. [PubMed: 17868091]
- Liu YB, Lio PA, Pasternak JF, Trommer BL. Developmental changes in membrane properties and postsynaptic currents of granule cells in rat dentate gyrus. *J Neurophysiol*. 1996; 76:1074–1088. [PubMed: 8871221]
- Lopez-Rojas J, Kreutz MR. Mature granule cells of the dentate gyrus--Passive bystanders or principal performers in hippocampal function? *Neurosci Biobehav Rev*. 2016; 64:167–174. [PubMed: 26949226]
- Lu B, Nagappan G, Guan X, Nathan PJ, Wren P. BDNF-based synaptic repair as a disease-modifying strategy for neurodegenerative diseases. *Nat Rev Neurosci*. 2013; 14:401–416. [PubMed: 23674053]
- McAllister AK, Lo DC, Katz LC. Neurotrophins regulate dendritic growth in developing visual cortex. *Neuron*. 1995; 15:791–803. [PubMed: 7576629]
- Meakin SO, MacDonald JI, Gryz EA, Kubu CJ, Verdi JM. The signaling adapter FRS-2 competes with Shc for binding to the nerve growth factor receptor TrkA. A model for discriminating proliferation and differentiation. *J Biol Chem*. 1999; 274:9861–9870. [PubMed: 10092678]
- Minichiello L, Calella AM, Medina DL, Bonhoeffer T, Klein R, Korte M. Mechanism of TrkB-mediated hippocampal long-term potentiation. *Neuron*. 2002; 36:121–137. [PubMed: 12367511]
- Mongiati LA, Esposito MS, Lombardi G, Schinder AF. Reliable activation of immature neurons in the adult hippocampus. *PLoS One*. 2009; 4:e5320. [PubMed: 19399173]
- Musumeci G, Sciarretta C, Rodriguez-Moreno A, Al Banchaabouchi M, Negrete-Diaz V, Costanzi M, Berno V, Egorov AV, von Bohlen Und Halbach O, Cestari V, Delgado-Garcia JM, Minichiello L. TrkB modulates fear learning and amygdalar synaptic plasticity by specific docking sites. *J Neurosci*. 2009; 29:10131–10143. [PubMed: 19675247]

- Nakashiba T, Cushman JD, Pelkey KA, Renaudineau S, Buhl DL, McHugh TJ, Rodriguez Barrera V, Chittajallu R, Iwamoto KS, McBain CJ, Fanselow MS, Tonegawa S. Young dentate granule cells mediate pattern separation, whereas old granule cells facilitate pattern completion. *Cell*. 2012; 149:188–201. [PubMed: 22365813]
- Nandi S, Gutin G, Blackwood CA, Kamatkar NG, Lee KW, Fishell G, Wang F, Goldfarb M, Hébert JM. FGF-Dependent, Context-Driven Role for FRS Adapters in the Early Telencephalon. *J Neurosci*. 2017; 37:5690–5698. [PubMed: 28483978]
- Neves G, Cooke SF, Bliss TV. Synaptic plasticity, memory and the hippocampus: a neural network approach to causality. *Nat Rev Neurosci*. 2008; 9:65–75. [PubMed: 18094707]
- Ohkubo Y, Uchida AO, Shin D, Partanen J, Vaccarino FM. Fibroblast growth factor receptor 1 is required for the proliferation of hippocampal progenitor cells and for hippocampal growth in mouse. *J Neurosci*. 2004; 24:6057–6069. [PubMed: 15240797]
- Patterson SL, Abel T, Deuel TA, Martin KC, Rose JC, Kandel ER. Recombinant BDNF rescues deficits in basal synaptic transmission and hippocampal LTP in BDNF knockout mice. *Neuron*. 1996; 16:1137–1145. [PubMed: 8663990]
- Pozas E, Ibanez CF. GDNF and GFR α 1 promote differentiation and tangential migration of cortical GABAergic neurons. *Neuron*. 2005; 45:701–713. [PubMed: 15748846]
- Ryan TJ, Roy DS, Pignatelli M, Arons A, Tonegawa S. Memory. Engram cells retain memory under retrograde amnesia. *Science*. 2015; 348:1007–1013. [PubMed: 26023136]
- Sahay A, Drew MR, Hen R. Dentate gyrus neurogenesis and depression. *Prog Brain Res*. 2007; 163:697–722. [PubMed: 17765746]
- Sholl DA. Dendritic organization in the neurons of the visual and motor cortices of the cat. *J Anat*. 1953; 87:387–406. [PubMed: 13117757]
- Smith DL, Pozueta J, Gong B, Arancio O, Shelanski M. Reversal of long-term dendritic spine alterations in Alzheimer disease models. *Proc Natl Acad Sci U S A*. 2009; 106:16877–16882. [PubMed: 19805389]
- Sultan S, Li L, Moss J, Petrelli F, Casse F, Gebara E, Lopatar J, Pfrieder FW, Bezzi P, Bischofberger J, Toni N. Synaptic integration of adult-born hippocampal neurons is locally controlled by astrocytes. *Neuron*. 2015; 88:957–972. [PubMed: 26606999]
- Super H, Martinez A, Del Rio JA, Soriano E. Involvement of distinct pioneer neurons in the formation of layer-specific connections in the hippocampus. *J Neurosci*. 1998; 18:4616–4626. [PubMed: 9614236]
- Sweet RA, Henteloff RA, Zhang W, Sampson AR, Lewis DA. Reduced dendritic spine density in auditory cortex of subjects with schizophrenia. *Neuropsychopharmacology*. 2009; 34:374–389. [PubMed: 18463626]
- Tonegawa S, Liu X, Ramirez S, Redondo R. Memory Engram Cells Have Come of Age. *Neuron*. 2015; 87:918–931. [PubMed: 26335640]
- Toni N, Schinder AF. Maturation and functional integration of new granule cells into the adult hippocampus. *Cold Spring Harb Perspect Biol*. 2015; 1:a018903.
- Turner CA, Watson SJ, Akil H. The fibroblast growth factor family: neuromodulation of affective behavior. *Neuron*. 2012; 76:160–174. [PubMed: 23040813]
- Uchida S, Teubner BJ, Hevi C, Hara K, Kobayashi A, Dave RM, Shintaku T, Jaikhan P, Yamagata H, Suzuki T, Watanabe Y, Zakharenko SS, Shumyatsky GP. CRTC1 Nuclear Translocation Following Learning Modulates Memory Strength via Exchange of Chromatin Remodeling Complexes on the Fgf1 Gene. *Cell Rep*. 2017; 18:352–366. [PubMed: 28076781]
- Wang HF, Shih YT, Chen CY, Chao HW, Lee MJ, Hsueh YP. Valosin-containing protein and neurofibromin interact to regulate dendritic spine density. *J Clin Invest*. 2011; 121:4820–4837. [PubMed: 22105171]
- Weeden CS, Roberts JM, Kamm AM, Kesner RP. The role of the ventral dentate gyrus in anxiety-based behaviors. *Neurobiol Learn Mem*. 2015; 118:143–149. [PubMed: 25498221]
- Zhao C, Teng EM, Summers RG Jr, Ming GL, Gage FH. Distinct morphological stages of dentate granule neuron maturation in the adult mouse hippocampus. *J Neurosci*. 2006; 26:3–11. [PubMed: 16399667]

- Zhu XN, Liu XD, Sun S, Zhuang H, Yang JY, Henkemeyer M, Xu NJ. Ephrin-B3 coordinates timed axon targeting and amygdala spinogenesis for innate fear behaviour. *Nat Commun.* 2016; 7:11096. [PubMed: 27008987]
- Zhuo L, Theis M, Alvarez-Maya I, Brenner M, Willecke K, Messing A. hGFAP-cre transgenic mice for manipulation of glial and neuronal function in vivo. *Genesis.* 2001; 31:85–94. [PubMed: 11668683]

Author Manuscript

Author Manuscript

Author Manuscript

Author Manuscript

Highlights

- FRS2 and FRS3 compensate for each other during postnatal brain development
- FRS adapters enhance stem cell numbers and neuron maturation in the dentate gyrus
- FRS adapters are required for dendritogenesis in postnatal dentate granule cells
- FRS adapters promote normal excitatory synaptogenesis in dentate granule cells

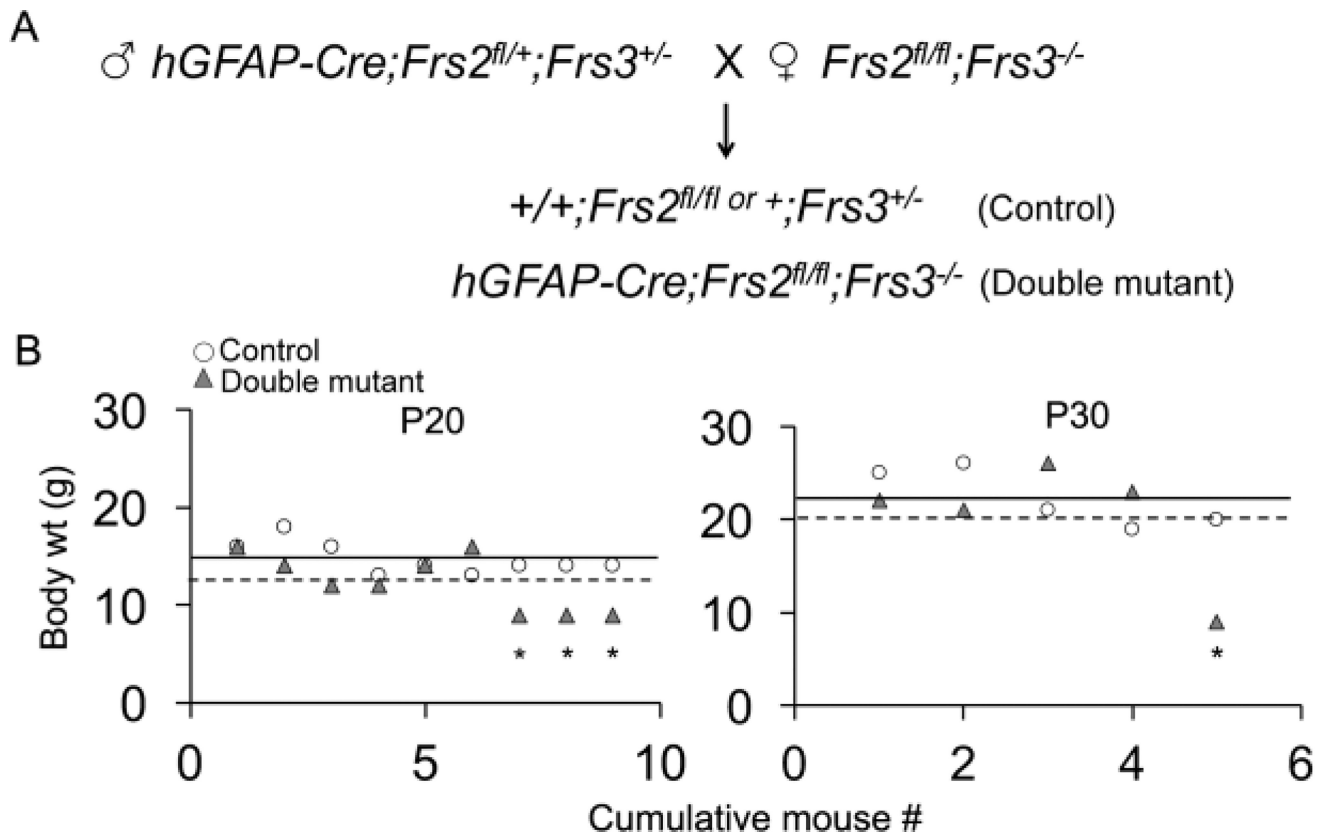


Figure 1. FRS regulates body weight and contributes to survival in a fraction of animals
 (A) Mating scheme for the generation of double mutant mice. (B) Reduced body weight in 33.3% of mutant mice at P20 (asterisks) and 20% of mutant mice at P30 (asterisk). Solid and broken lines respectively indicate average body weights of control and mutants. $n=9$ (P20) and $n=5$ (P30). About 13.3% of all mutant mice (with lower body weights) died between P20 and P30 and the other 20% (also with lower body weights) died ~P60–P75. None of the mutant mice with normal body weights or control group displayed any sign of mortality.

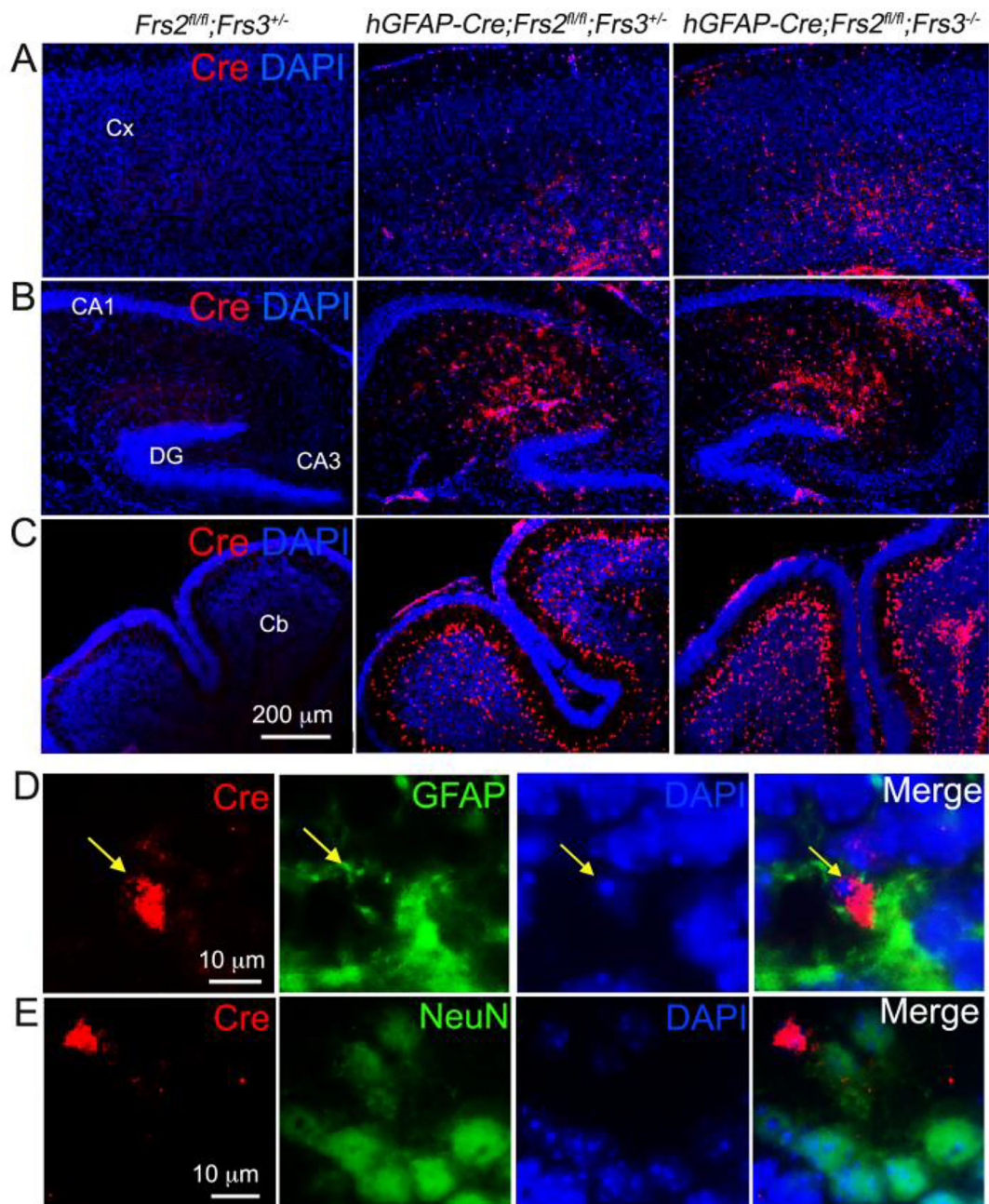


Figure 2. Expression of the *hGFAP-Cre* transgene is not affected by the loss of *Frs3*
 (A–C) IHC analyses of P7 brain sections for the detection of Cre expression in cortex (A), hippocampus (B) and cerebellum (C) on a *Frs2^{fl/fl};Frs3^{+/-}* (*Frs3* control) and *Frs2^{fl/fl};Frs3^{-/-}* (*Frs3* mutant) genetic backgrounds. Counterstain, DAPI. n=2. Cx, Cortex; DG, dentate gyrus; Cb, cerebellum. (D–E) Cre expression in the DG. IHC analyses of P7 *hGFAP-Cre;Frs2^{fl/fl};Frs3^{+/-}* brain sections through DG showing Cre expression in GFAP+ (D, arrow) but not in NeuN+ cells (E). Counterstain, DAPI.

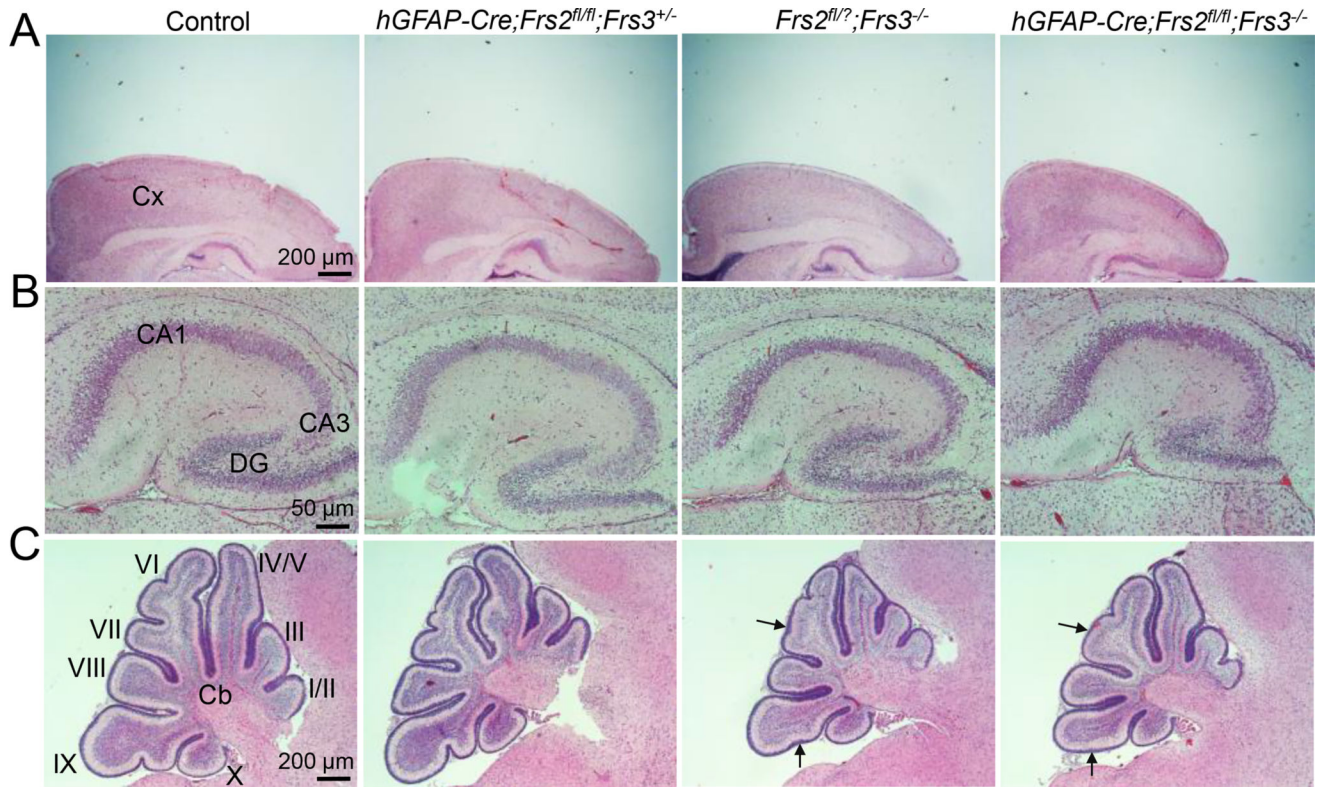


Figure 3. FRS2 and FRS3 collaborate during postnatal brain development

(A–C) Photomicrographs of sagittal H&E stained brain sections from P7 mice showing smaller brains along the A/P axis in double mutants compared with either control or single mutants. Despite a reduced size along the A/P axis, the cortical thickness was largely normal in double mutants (A). The DG was particularly reduced in double mutants (B). Cerebellar foliation deficits (lobes VI/VII and IX) were observed in *Frs3* single as well as in double mutants (C, arrows). Note, *Frs2* single mutants displayed a largely normal brain development even on a *Frs3*^{+/-} background. n=3. Cx, Cortex; DG, dentate gyrus; Cb, cerebellum.

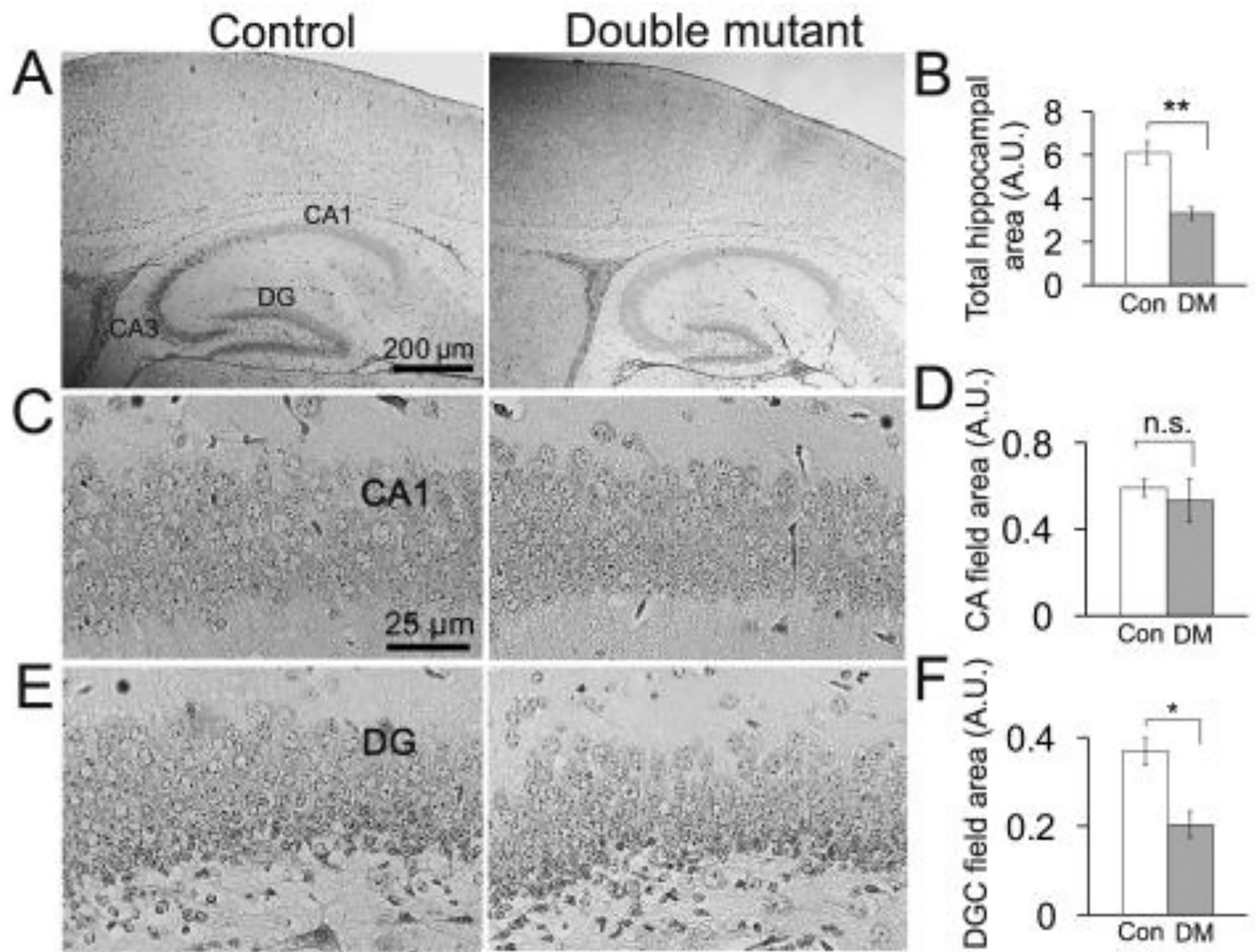


Figure 4. FRS is required for DG morphogenesis

(A,C,E) Photomicrographs of sagittal H&E stained brain sections from P7 mice showing a smaller hippocampus with altered DG morphogenesis (A), a normal CA1 neuronal field area (C), and a reduced DGC field area (E) in mutants. (B,D,F) Quantitation of fields of 5× (A) or 40× (C,E) images from three consecutive equivalent sagittal planes derived from serially cut 5 μm thick sections from three mice per genotype was carried out for comparison. A.U., arbitrary units. Average ± SEM. Unpaired two-tailed Student's t-test was used. n.s., non-significant; *p<0.05. Con, control; DM, double mutant.

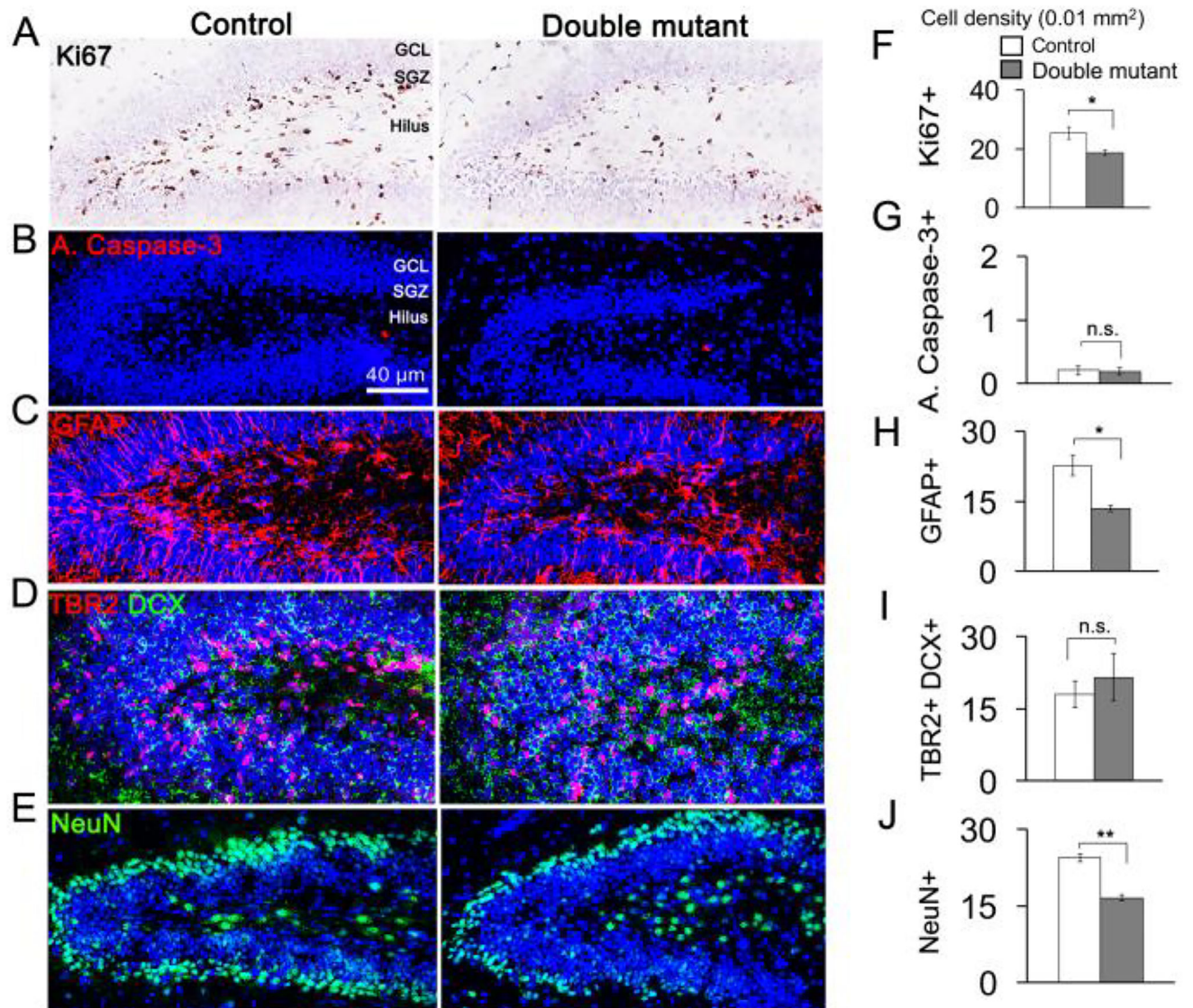


Figure 5. FRS promotes DG neural stem cell proliferation and DGC maturation

(A–E) Double mutant mice exhibited reduced neural stem cell proliferation and a reduced number of mature neurons. IHC analyses of P7 brain sections through the DG for markers of proliferation, Ki67 (A); cell death, active caspase-3 (B); neural stem cells, GFAP (C); immature neurons, DCX and TBR2 (D); and mature DGCs, NeuN (E). Counterstain, hematoxylin (A) and DAPI (B–E). (F–J) Quantitation for (A–E). Twenty-four different fields from three mice per genotype were analyzed. Average \pm SEM. Unpaired two-tailed Student's t-test was used. n.s., non-significant; * $p < 0.05$ and ** $p < 0.01$.

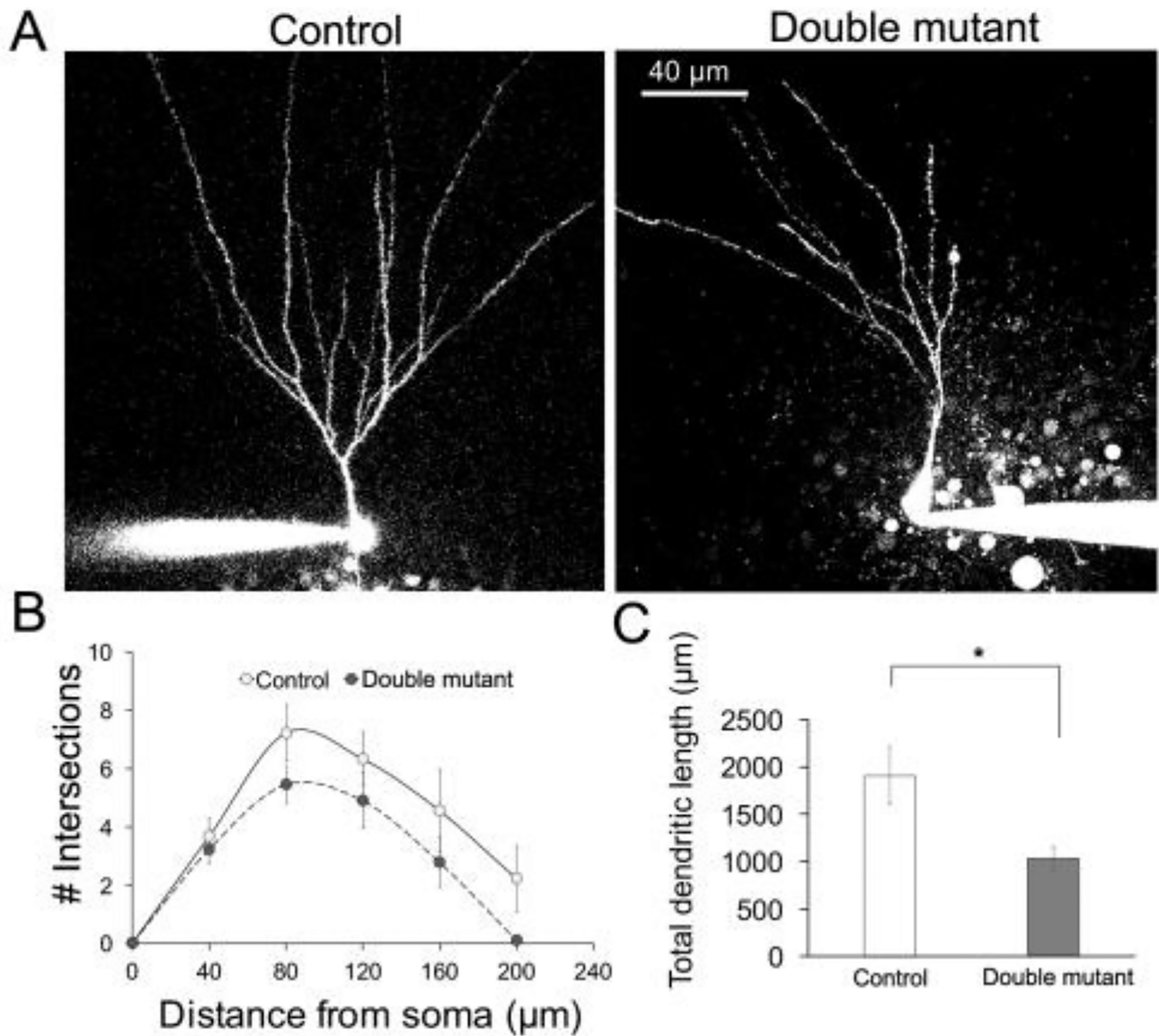


Figure 6. FRS is required for DGC dendritic branching

(A–B) Double mutant mice exhibited reduced DGC dendritic arborization. Mutant mice with lower body weights at P20 were excluded from these analyses. Soma of single DGCs located at least 30 μm above the hilar border in acute hippocampal slices from P21–P25 mice were patched-loaded with Alexa Fluor-594 (30 μM) for two-photon imaging of morphology. Traces of reconstructed DGC dendritic trees by concentric 40 μm bins from the soma using Neurolucida neuron tracing software were used for Sholl analyses. Imaged cells (A). Sholl analysis quantitation (B). Data points corresponding to 200 μm distance from cell body were excluded from statistical analyses due to the lack of sufficient data points in mutants. Average \pm SEM. Two-way ANOVA was used (B). $F_{1,33}=4.58$; $p=0.04$. (C) Double mutant mice exhibited reduced total DGC dendritic tree length. At least ten different DGCs from five mice per genotype were analyzed. Average \pm SEM. Unpaired two-tailed Student's *t*-test was used (C). * $p<0.05$.

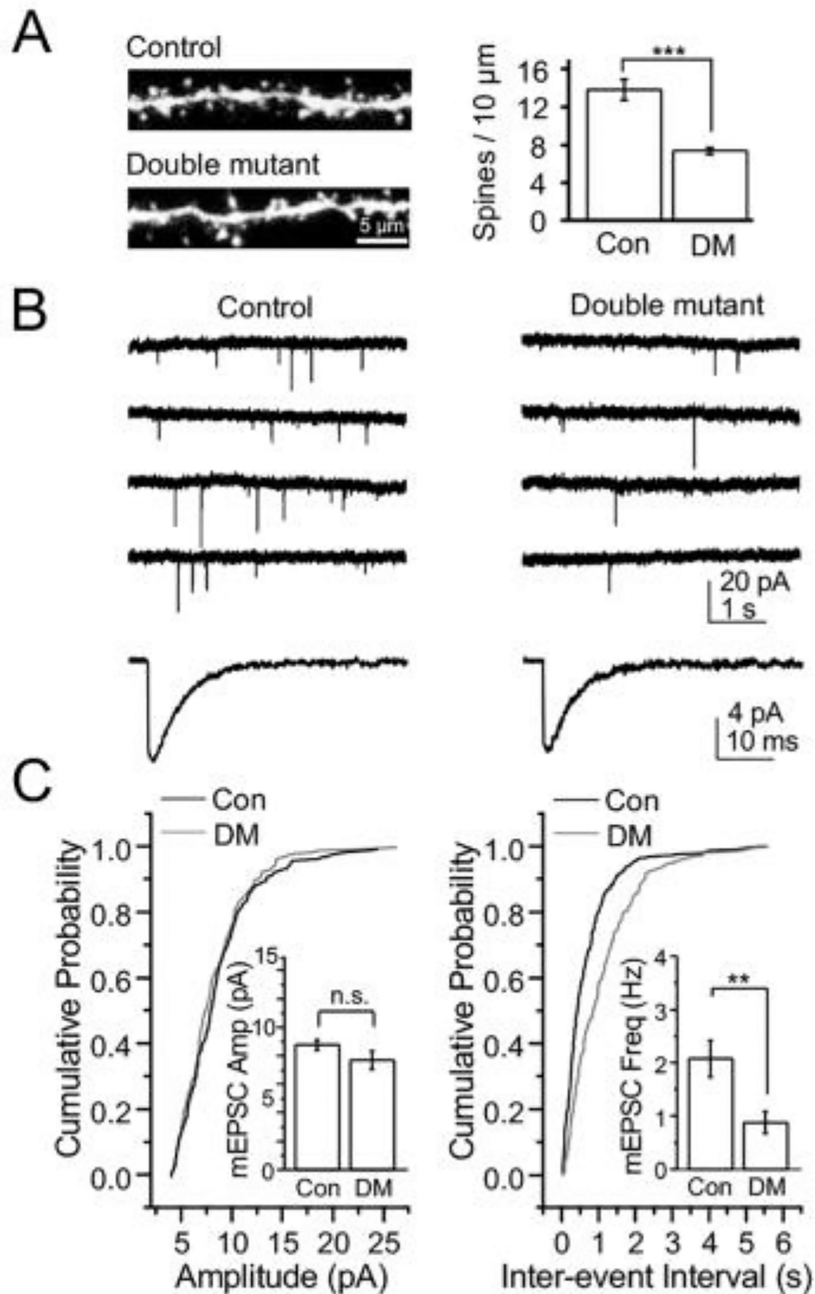


Figure 7. FRS is required for excitatory synaptogenesis in DGCs

(A) Double mutant mice exhibited reduced DGC dendritic spine density. Mutant mice with lower body weights at P20 were excluded from these analyses. Spines located in the dendrites at a distance 50 μm from the soma were imaged at higher resolution and magnification as described in the Materials and Methods. Spine density was assessed using the Image J software. Twenty different dendrites of ten different cells from five mice per genotype were used for spine density analyses. Average \pm SEM. Unpaired two-tailed Student's *t* test was used. (B-C) Double mutant DGCs exhibited a reduction in frequency but not amplitude of mEPSCs. Synaptic events were recorded from DGCs of P21–P25 mice in

the presence of 100 μM picrotoxin and 0.5 μM TTX. Four representative mEPSC sweeps from control and mutant DGCs (B, Upper). Composite average of mEPSC events (B, Lower). Cumulative probability plots of mEPSC amplitudes (left) and inter-event intervals (right) (C). Insets, summary histograms for mean amplitude (left) and frequency (right). At least eight different cells from three mice per genotype were considered. Average \pm SEM. One-way ANOVA was used. n.s., non-significant; ** $p < 0.01$ and *** $p < 0.001$. Amp, Amplitude; Freq, frequency; Con, Control; DM, double mutant.